

# A Heterogeneous Domain Decomposition Method for the Full Wave Analysis of Complex Airborne Antenna Systems

Zhen Peng <sup>#1</sup>, Kheng-Hwee Lim <sup>\*2</sup>, Jin-Fa Lee <sup>#3</sup>

<sup>#</sup> *ElectroScience Lab, The Ohio State University  
1330 Kinnear Road, Columbus, OH 43212, USA*

<sup>1</sup> peng.98@osu.edu

<sup>3</sup> lee.1863@osu.edu

<sup>\*</sup> *DSO National Laboratories*

*20 Science Park Drive Singapore 118230*

<sup>2</sup> lkhenghw@gmail.com

**Abstract**—A heterogeneous domain decomposition method is presented for efficiently and effectively analyzing the antenna and radome mounted on a realistic airborne platform. The proposed non-conformal domain decomposition method follows a hierarchical domain partitioning strategy. The entire computational domain is decomposed into non-overlapping sub-regions. A surface integral equation domain decomposition method is applied for the full wave solution of the homogeneous sub-regions, such as airborne platform. A non-conformal finite element domain decomposition method is proposed for solving sub-regions involving significant repetitions: such as large finite antenna arrays, frequency selective surfaces, and metamaterials. To further improve the convergence in the DDM iterations, an optimal 2nd order transmission condition is introduced to enforce field continuities across domain interfaces. A complex airborne antenna system-level simulation is conducted to illustrate the potential benefits offered by the proposed method.

**Index Terms**—Maxwell's equations, antenna array, integral equation method, finite element method, domain decomposition method.

## I. INTRODUCTION

Large finite antenna arrays are commonly used in airborne platforms to transmit and receive signals through spaces. As shown in Fig. 1, an interlaced dual periodic antenna array is installed on the nose section of an aircraft serving for wireless communications. The objective of this work is to perform the full wave analysis to study the performance of large finite antenna arrays and radome when mounted on platforms with realistically complex shapes and materials. Such a task involves multiple technical difficulties that greatly tax the capability of existing numerical techniques such as: finite element [1], finite difference, integral equation methods [2], [3], hybrid methods [4], [5] etc., in terms of the desired accuracy, modularity and the stability of mathematical formulations.

One of the major difficulties comes from the modeling of the finite antenna arrays, which has both large problem size due to the large number of antenna elements and geometrically complicated structures that involve complex materials. In order to accurately evaluate the performance of the installed antenna

arrays, both there surrounding regions and the platform need to be included in the computational domain. Taking the featured problem depicted in Fig. 1 for instance, the nose radar array is comprised of 584 horizontally polarized Vivaldi antenna elements, operated at 10 GHz; and, of particular concern is that this array is mounted on a complicated repositioner to perform mechanically scanning to widen its field of view. Moreover, a hollow composite radome with frequency selective surface (FSS) is located at the front of the array to protect antenna from the exterior environment. Both repositioner and radome are adjacent to the main fuselage of the aircraft. Full wave analysis of such a large multi-scale problem is extremely challenging and is possibly beyond the capabilities of conventional numerical methods, which is the major motivation of this work.

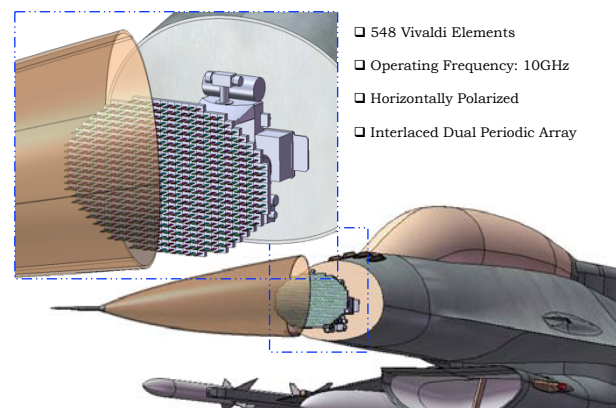


Fig. 1. An interlaced dual periodic array installed on aircraft.

## II. METHODOLOGY

Recently, finite element based non-overlapping domain decomposition methods (FE-DDM) [6]–[8] have been very popular for solving electromagnetic problems with significant repetitions. Particularly, a non-overlapping and non-conformal

FE-DDM is presented for modeling large finite antenna arrays [9]. The non-conformal property permits the use of completely independent discretization for each of the sub-domains. A mixed true second order transmission condition (SOTC) with corner edge penalty terms is developed to facilitate fast convergence in the DDM iterations. Furthermore, a finite element tearing and interconnecting (FETI) [10], [11] sub-structuring strategy is utilized to exploit local repetitions and also local rotational and translational symmetries within the large antenna array. This results in a considerably reduced problem involving only the surface unknowns at the skeleton of the domain interfaces. The computational resources can be drastically reduced.

Despite these advances, we still find it is difficult and expensive to solve the problem shown in Fig. 1. In the previous work [9], the first order absorbing boundary condition (ABC) is applied to truncate the computational domain, which produces the unwanted spurious reflection from the truncation boundary. In order to minimize such unphysical reflection, the truncation boundary must be convex in shape and placed sufficiently far away from the arrays, resulting in a larger computational domain. Furthermore, the use of absorbing boundary condition may not be adequate as an accurate mesh truncation method in this study. Since our goal is to allow accurate analysis of the installed performance of antenna arrays, the EM interactions between the antenna array, radome, and platform have to be accurately represented. The truncation boundaries using ABC alter the physical character of the problem and fails to represent the exterior space correctly.

In this work, we present a heterogeneous domain decomposition method for the full wave analysis of installed antenna arrays on realistic platforms. Recognizing that the entire computational domain involves an complicated antenna array embedded in an exterior unbounded space, we propose to treat the unbounded space exterior to the antenna array as an additional domain, which is formulated by surface integral equation method. The use of the surface integral method [4], [5] etc.), arguably, offers the best accuracy for modeling unbounded electromagnetic radiation and scattering problems, albeit at the increases of memory and CPU times. To further improve the capability of the proposed method, surface integral equation domain decomposition method (SIE-DDM) is introduced for the solution of the exterior unbounded space [12]. Consequently, the proposed domain decomposition scheme follows a hierarchical domain partitioning strategy, as illustrated as follows:

- Level 1: Non-conformal DDM between the interior antenna array and exterior region. The entire computational domain is decoupled as two computational domains, namely, a finite domain encloses the antenna array inside and the space exterior to the antenna array. The aim is to combine FEM's versatility and robustness to model geometrically complex structures and spatially varying materials and also the SIE's ability to efficiently and accurately solve unbounded domains.
- Level 2: Computational Partitioning for interior com-

plicated structures and exterior region. For the interior FEM region involving locally repetitive structures, we proceed to partition it into non-overlapping sub-domains. The FETI method is employed to take advantage of the repetitions to drastically reduce the computational resources. Since the exterior region consists of piecewise homogeneous sub-regions, the SIE-DDM is an appealing full wave approach. The proposed SIE-DDM starts by partitioning the exterior region into homogeneous sub-domains with homogeneous material properties. Each local sub-domain is enclosed as a closed surface and a generalized combined field integral equation (G-CFIE) is employed as sub-domain solver.

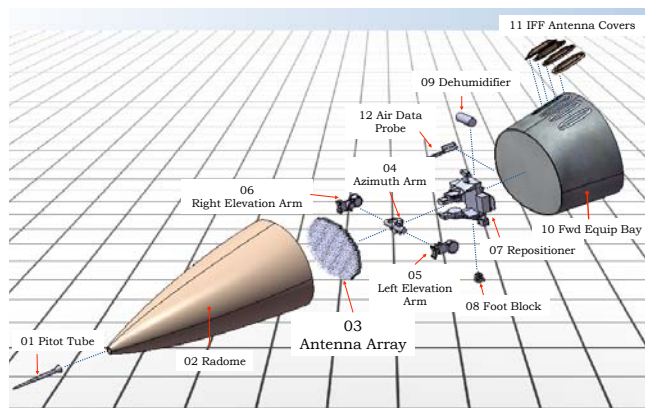


Fig. 2. A hierarchical domain partitioning for complex airborne antenna system

The major technical ingredients of the proposed heterogeneous domain decomposition method include:

- *Multiple Electric and Magnetic Traces.* Through this decomposition, we have defined multiple electric and magnetic traces on the interior side as well as the exterior side of the sub-region surface. This multiple-traces feature admits two major benefits: Interior FE-DDM and exterior SIE-DDM sub-domains can be modularly treated in terms of domain partitioning, discretization, preconditioning, and solution process. This provides flexibility for design and parameter studies, since it is possible to modify the portion of the geometry and materials that have changed during the design process. Moreover, there is no need to generate a conformal discretization of the entire exterior boundary of target.
- *Optimized Second Order Transmission Condition.* We propose herein an optimized second order transmission condition, which chooses the optimal values based on the sub-domain size, the mesh density and the problem size. It will result in a coercive and convergent DD algorithm. The performance of such scales very well with respect to  $kh$  (mesh size),  $kd$  (the electric size of the sub-domain), as well as  $kD$  (the electric size of the entire problem domain).
- *Generalized Combined Field Integral Equation.* The generalized CFIE formulation, which is comprised of tangen-

tial components of both electric and magnetic fields, is derived to guarantee the removal of the resonance solution and yields accurate and stable numerical solutions. It also offers one very distinctive feature. Namely, when the boundary of the sub-domain is formed completely by PEC, the formulation automatically reduces to the classical CFIE formulation for PEC closed targets.

### III. NUMERICAL RESULTS

#### A. Large Finite Antenna Array

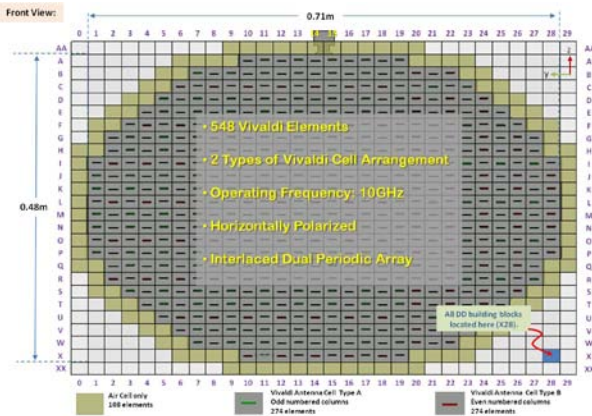


Fig. 3. An interlaced dual periodic antenna array layout

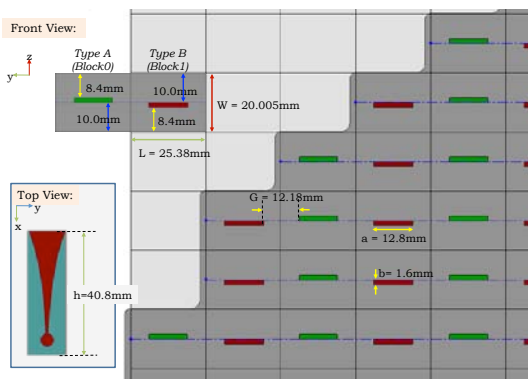
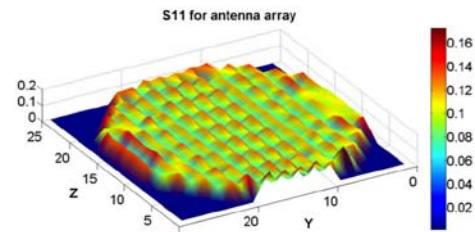


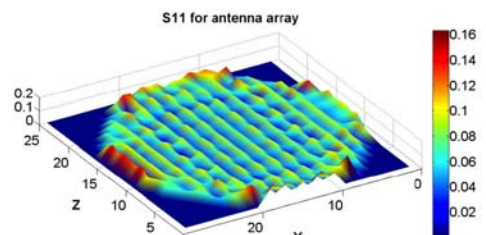
Fig. 4. Geometric description of the antenna array.

Shown in Fig. 3 and Fig. 4 is a nose radar antenna array, which is made of 548 Vivaldi antenna elements, operating at the X-band. We first applied the FETI technique to solve for the antenna elements numerical transfer function. With the numerical transfer function available for the Vivaldi antenna element, we proceed to model the entire antenna array using two solution procedures: (a) A FE-DDM with 2nd order optimal transmission condition and with the absorbing boundary condition placed  $0.5 \lambda$  away from the array. It was denoted as the FE-DDM-ABC in the figure; and, (b) By combining the FE-DDM and the G-CFIE method, we form automatically a hybrid finite element boundary integral (FEBI) formulation to model the antenna array. For the nose radar antenna array, it took only 8 iterations using the general conjugate residual

(GCR) Krylov matrix solution to converge with a relative residual less than  $10^{-3}$  for the FE-DDM-ABC. Whereas the hybrid FE-DDM with the G-CFIE, we employed the inner-outer loop iteration strategy and it took total 5 outer loop iterations, inner loop tolerance set to  $10^{-3}$ , to have the global residual converged to less than  $10^{-2}$ . Comparisons of the computed  $S_{11}$  parameters of all the antenna elements are included in Fig. 5. The results computed from the hybrid FE-DDM with G-CFIE do show noticeable differences from the FE-DDM-ABC results. Finally, in Fig. 6, we plotted the antenna patterns calculated using the two methods. We note that there is a significant difference at the side lobe, due to the fact that FE-DDM-ABC fails to accurately model the surface wave propagating along the surface of the array.



(a) FE-DDM-ABC



(b) Hybrid FE-DDM with G-CFIE

Fig. 5.  $S_{11}$  parameters of all the antenna elements.

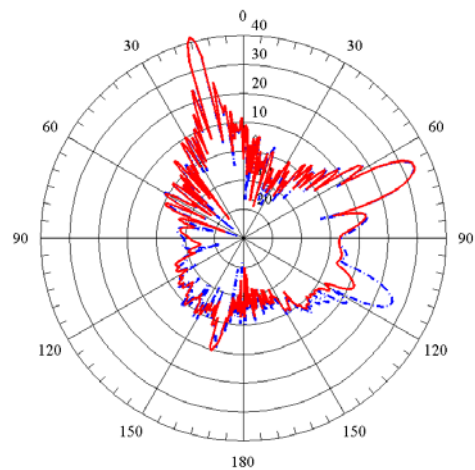


Fig. 6. Radiation pattern of antenna array with scanning angle  $15^\circ$ . Blue dash line: FE-DDM-ABC; Red solid line: hybrid FE-DDM with G-CFIE



### B. Installed Finite Antenna Array on Airborne Platform

We proceed to analyze the installed performance of the antenna array on a complicated airborne platform, operating at X-band. Two type of radomes will be mounted at the front of the array. One is a single-layer dielectric radome with 10mm thickness and permittivity (4.8,  $-0.0096$ ). The other radome is a honeycomb composite structure while the permittivity of the honeycomb core is (3.8,  $-0.0076$ ) and the thickness of the honeycomb is 10mm. The size of the honeycomb cell is  $5.3\text{mm} \times 3.5\text{mm}$  and the total number of honeycomb cells is 88,000. Considering the complexity of the problem, the SIE-DDM is applied for the full wave solution of the exterior region. Following the strategy of the proposed heterogeneous DDM, the entire model is divided into 21 surface integral equation sub-domains and 556 finite element sub-domains. It took total 17 outer loop iterations to have the global residual converged to less than  $10^{-2}$ . The electric current distributions of the complex airborne antenna system with two radome configuration are depicted in Fig. 7 and Fig. 8. Finally, we plot the radiation patterns of the two installed antenna arrays. Comparing to the free standing Vivaldi antenna array, the performances of the installed array are significantly altered due to the imperfect design of the radome. The use of the honeycomb composite radome considerably improves the performance of the installed array.

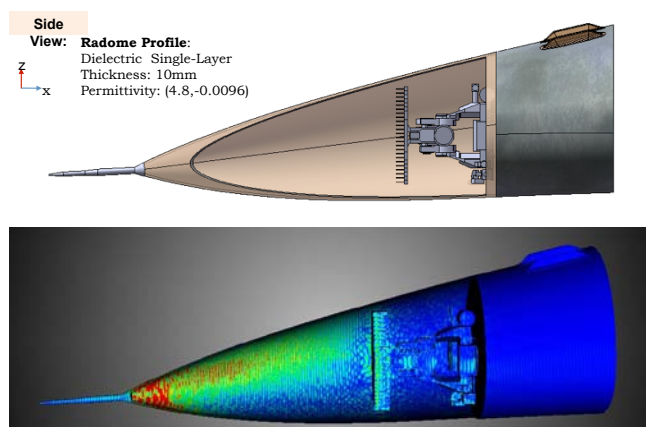


Fig. 7. Electric current distribution of a complex airborne antenna system.

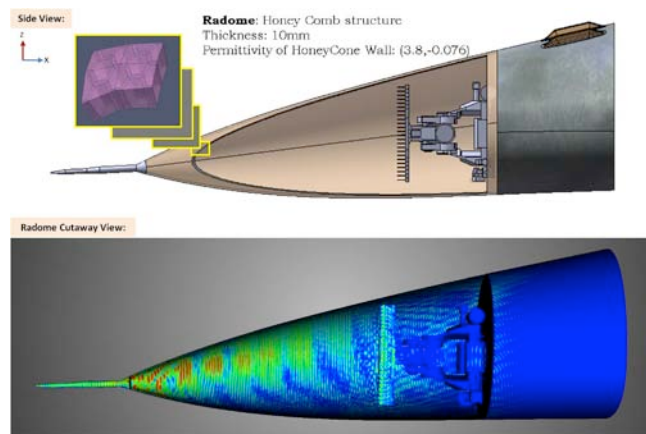


Fig. 8. Electric current distribution of a complex airborne antenna system.

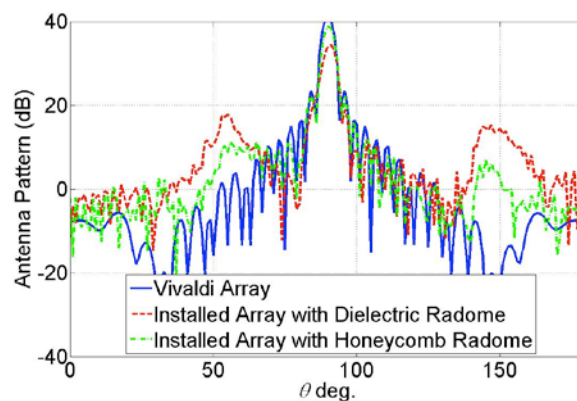


Fig. 9. Radiation pattern of installed finite antenna array on airborne platform.

### REFERENCES

- [1] J. Liu and J. Jin, "Scattering analysis of a large body with deep cavities," *IEEE Trans. Antennas and Propagation*, vol. 51, no. 6, pp. 1157–1167, June 2003.
- [2] S. Seo and J.-F. Lee, "A fast ie-fft algorithm for solving pec scattering problems," *IEEE Trans. Magnetics*, vol. 41, no. 5, pp. 1476–1479, May 2004.
- [3] F. Andriulli, K. Cools, F. Olyslager, A. Buffa, S. Christiansen, and E. Michielssen, "A multiplicative calderon preconditioner for the electric field integral equation," *IEEE Trans. Antennas and Propagation*, vol. 56, no. 8, pp. 2398–2412, Aug. 2008.
- [4] B. Stupfel, "A hybrid finite element and integral equation domain decomposition method for the solution of the 3-D scattering problem," *J. Comput. Phys.*, vol. 172, pp. 451–471, Sept. 2001.
- [5] M. Vouvakis, K. Zhao, S.-M. Seo, and J.-F. Lee, "A domain decomposition approach for non-conformal couplings between finite and boundary elements for electromagnetic scattering problems in  $\mathbb{R}^3$ ," *J. Comput. Phys.*, vol. 225, pp. 975–994, 2007.
- [6] Y.-J. Li and J.-M. Jin, "A new dual-primal domain decomposition approach for finite element simulation of 3-D large-scale electromagnetic problems," *IEEE Trans. Antennas and Propagation*, vol. 55, no. 10, pp. 2803–2810, Oct. 2007.
- [7] K. Zhao, V. Rawat, S.-C. Lee, and J.-F. Lee, "A domain decomposition method with nonconformal meshes for finite periodic and semi-periodic structures," *IEEE Trans. Antennas and Propagation*, vol. 55, no. 9, pp. 2559–2570, Sept. 2007.
- [8] Z. Peng and J.-F. Lee, "Non-conformal domain decomposition method with second-order transmission conditions for time-harmonic electromagnetics," *J. Comput. Phys.*, vol. 229, no. 16, pp. 5615–5629, 2010.
- [9] —, "Non-conformal domain decomposition method with mixed true second order transmission condition for solving large finite antenna arrays," *IEEE Trans. Antennas and Propagation*, vol. 59, no. 5, pp. 1638–1651, May. 2011.
- [10] C. Farhat and F.-X. Roux, "A method of finite element tearing and interconnecting and its parallel solution algorithm," *Internat. J. Numer. Methods Engrg.*, vol. 0, no. 0, pp. 1205–1227, 1991.
- [11] Y.-J. Li and J.-M. Jin, "A vector dual-primal finite element tearing and interconnecting method for solving 3-D large-scale electromagnetic problems," *IEEE Trans. Antennas and Propagation*, vol. 54, no. 10, pp. 3000–3009, Oct. 2006.
- [12] Z. Peng, X.-C. Wang, and J.-F. Lee, "Integral equation based domain decomposition method for solving electromagnetic wave scattering from non-penetrable objects," *IEEE Trans. Antennas and Propagation*, vol. 59, no. 9, pp. 3328–3338, Sep. 2011.